Performance Improvements in Solid Fuel Microthrusters

ROBERT J. VONDRA*
Massachusetts Institute of Technology, Lincoln Laboratory, Lexington, Mass.
AND
KEITH I. THOMASSEN†
Massachusetts Institute of Technology, Cambridge, Mass.

The performance of 2- and 20-joule pulsed electric thrusters with a new fuel feed system is investigated. A theoretical model is developed to explain measurements of the specific impulse and impulse bit when geometric variations are made to optimize performance. An improvement in either specific impulse or impulse bit and in efficiency is found over the conventional back-fed thruster. Effects of electrode geometry on performance and on ablation patterns are noted. A study of the breakdown electric field patterns and subsequent Hall current paths is invoked to explain the observations.

Introduction

SOLID fuel pulsed plasma thrusters are currently under investigation for their use in satellite control. At present, both attitude control and east-west stationkeeping[1] can be achieved with these thrusters. Future use for N-S stationkeeping and station changing requires improvements in lifetimes, efficiency, and thrust. Consequently, after a long diagnostic program[2,3] to understand the operation of the LES-6 (Lincoln Experimental Satellite) thrusters (Fig. 1), a program to improve the performance of these thrusters has begun.

This report describes several experiments to increase the efficiency and impulse bit at a given energy by a variety of geometrical changes in the fuel feed, electrode configuration, and electrode transition to the capacitor. In particular, Teflon fuel bars are fed from each side of the discharge arc rather than from the back, as in the LES-6 thrusters. By varying the spacing between the two bars, one can control the mass ablated per shot, which in turn varies the specific impulse I_{sp} and impulse bit I_{bit} in agreement with the theory given here. Thruster performance can therefore be optimized.

Finally, uneven ablation of the Teflon is observed, as are carbon deposits on a portion of the Teflon faces. Since this presents problems for the continuous feeding and consumption of the fuel bars, a hypothesis is advanced to explain the origin of these patterns and a remedy is suggested.

Side Feed Thruster

The side feed thruster analyzed in this paper is shown schematically in Fig. 2. It is similar in operation to the LES-6 thruster of Fig. 1, differing only in the fuel feed and flared electrodes used on some of the experiments. This feed arrangement allows the two 1 in. × 1 in. × 8 in. bars to be used from one spark plug, saving weight and simplifying the electronics. Both 2- and 20-joule storage capacitors were used in the tests.

In the experiments described later in the text, the distance d between fuel faces is varied between $\frac{1}{8}$ in. and 1 in., resulting in a variation of mass per shot over a nearly 2–1 range. Since the theory which follows predicts a variation with mass in I_{sp}, I_{bit}, and efficiency η, we can obtain arbitrary per-

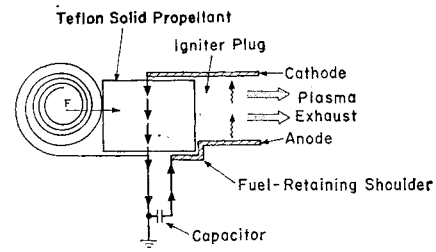

Fig. 1 Schematic of the LES-6 pulsed plasma thruster. The igniter plug initiates the discharge of the 2μF capacitor across the Teflon face. A negator spring feeds Teflon into the nozzle as fuel is consumed.

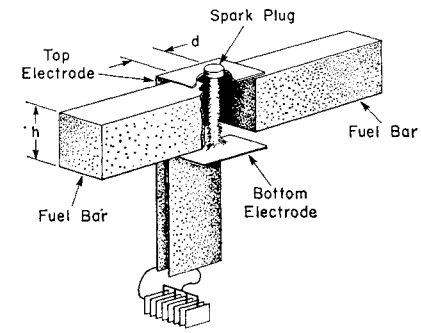

Fig. 2a Side feed thruster with parallel electrodes.

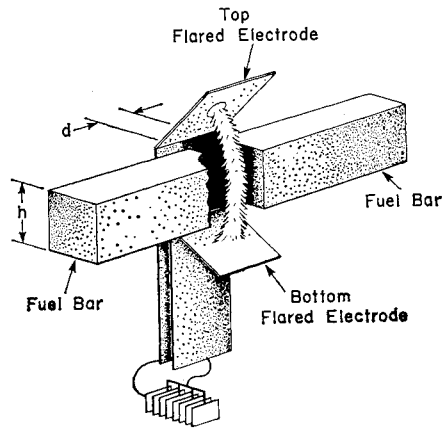

Fig. 2b Side feed thruster with flared electrodes.

Presented as Paper 72-210 at the AIAA 10th Aerospace Sciences Meeting, San Diego, Calif., January 17–19, 1972; submitted February 2, 1972; revision received May 26, 1972. This work was sponsored by the Department of the Air Force.
Index category: Electric and Advanced Space Propulsion.
* Staff Member. Member AIAA.
† Associate Professor, Electrical Engineering.

formance parameters (within limits) by choosing the spacing. One purpose of this paper is to verify this prediction.

Theory

Consider first the following theoretical model for calculating the thrust of the device. There are two contributions to the net force on the plasma exhaust, the magnetic and gas-dynamic forces. These are calculated by surrounding the entire exhaust by an imaginary surface and integrating the magnetic and gas-dynamic stresses on that surface. If we assume the stresses act largely on the area of height h and width w behind the arc, then the pressures are easily determined with some simplifying assumptions.

The total impulse from the magnetic pressure is

$$I_{\text{mag}} = \iiint_0^\infty \frac{\mu_0 H^2}{2} dA\, dt \approx \frac{1}{2}\mu_0 \frac{h}{w} \int_0^\infty I^2(t)\, dt$$

Since the arc width is determined largely by plasma processes (it is not equal to the fuel spacing), and the integrated current mainly by the stored energy and circuit parameters, this term is essentially independent of mass. The gas-dynamic contribution from the pressure is

$$I_{\text{gas}} = \iint dA \int_0^t nm\langle v_i v_j \rangle\, dt$$

$$\approx \sum_\alpha m_\alpha c_\alpha$$

where m_α and c_α are the mass and average thermal velocity of each species. (Earlier experiments[4] showed that there are many ion species in the exhaust.) The thermal velocities are also governed primarily by plasma processes, so they should be insensitive to changes in the exhaust mass.

According to this simple model, the total impulse bit is

$$I_{\text{bit}} = \frac{\mu_0 h}{2w} \int I^2\, dt + m\bar{c} \tag{1}$$

where $\bar{c}$ is the mass averaged thermal velocity, averaged over the contributing species. Then the specific impulse is

$$I_{\text{sp}} = I_{\text{bit}}/mg = I_{\text{mag}}/mg + \bar{c}/g \tag{2}$$

Efficiency is given by

$$\eta = g\frac{I_{\text{bit}} I_{\text{sp}}}{2E} = \frac{I_{\text{bit}}^2}{2mE} = \frac{m}{1}\cdot\frac{I_{\text{mag}}^4}{2E} + m\cdot\frac{\bar{c}^2}{2E} + \frac{I_{\text{mag}}\bar{c}}{E} \tag{3}$$

where E is the energy stored in the capacitor and g is the gravitational constant. Note that the first term on the right is proportional to m^{-1}, the second term proportional to m and the third term is independent of m. An alternative derivation of these equations, also predicting this mass dependence, was given by Solbes and Vondra.[5]

The approximations made here are obvious, and one can argue that these results are only semiquantitative. Nonetheless, the gross features should be correct, particularly the mass dependence. With this theory as a framework, one can proceed with the experimental test.

Side Feed Performance

Measurements of the average impulse bit were made on a pendulum-type thrust stand used by Radley[6] and described in earlier papers[2,3] for various fuel separation distances d (see Fig. 2a). After each measurement, the fuel and electrode weights were compared with their initial weights, and the average mass per shot was determined. The electrode erosion was negligible except at very large separation distances. Data was not used at separations for which the erosion of the electrode contributed as much mass as did the Teflon fuel. These measurements were made for both 2- and 20-joule energies, with both parallel and flared (90°) nozzles.

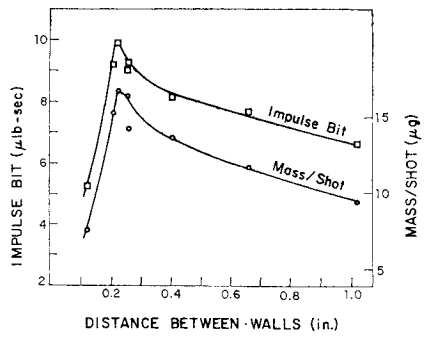

Fig. 3 I_{bit} and mass/shot for 2-joule side feed thruster.

In Fig. 3, the measured impulse bit and the mass per shot are plotted vs distance between fuel faces for a 2-joule thruster with a flared nozzle. The solid curves are the best "eyeball" fit to the data. Similar results are shown in Fig. 4 using a 20-joule capacitor on the same thruster. As stated earlier, the mass per shot varies with spacing; hence, we have control over this parameter.

Since the specific impulse and efficiency are both determined from the data of Figs. 3 and 4, these same data points can be plotted as in Figs. 5 and 6, respectively, for the 2-joule and 20-joule thrusters with mass as the independent variable. The solid curves now have the mass dependence given by the theory, and are fitted by eye in the regions where data were taken. These curves, of course, are not independent, so all curves fit the data equally well.

Very little difference in performance is found with parallel electrodes as Fig. 7 shows. Here, larger spacings were used to obtain data at low mass consumption to verify the improvement in efficiency. However, electrode erosion is severe at this spacing, as explained earlier. Of interest here is the 3–1 range in I_{bit} and the 5–1 range in I_{sp} available for different spacings.

Figures 5–7 show strong support for the simple model by verifying the mass dependence. Furthermore, calculations for I_{mag} from this model using the measured current waveform are known to give correct values for this contribution to the thrust (see Ref. 2). Thus, the intercept of I_{bit} at zero mass can be predicted fairly well from independent measurements.

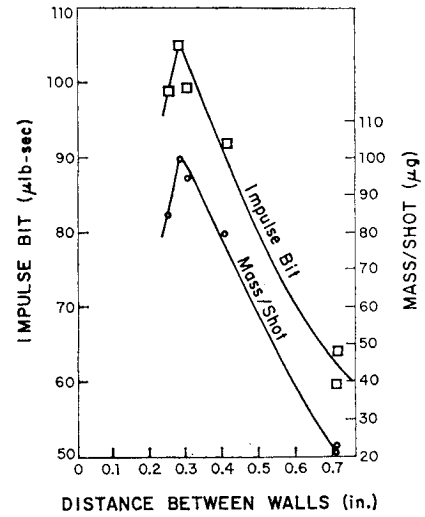

Fig. 4 I_{bit} and mass/shot for 20-joule side feed thruster.

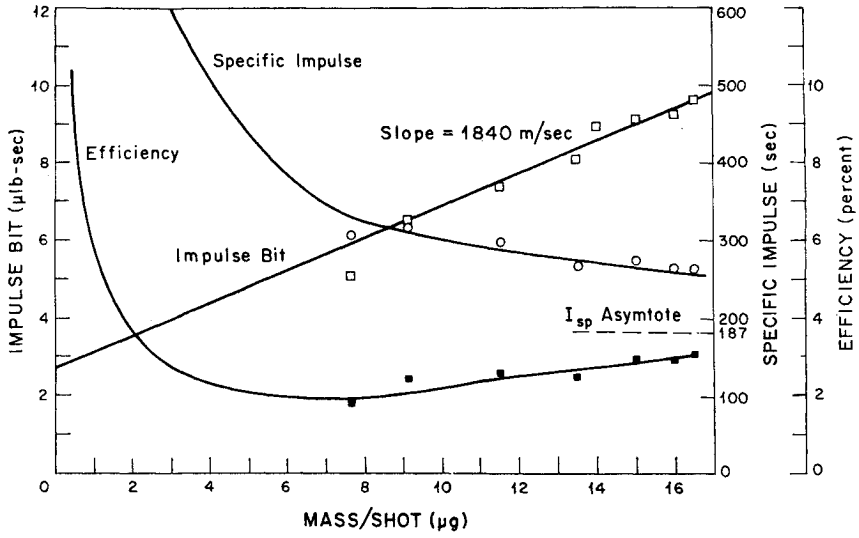

Fig. 5 Performance of 2-joule side feed thruster (with flared electrodes) as a function of mass/shot.

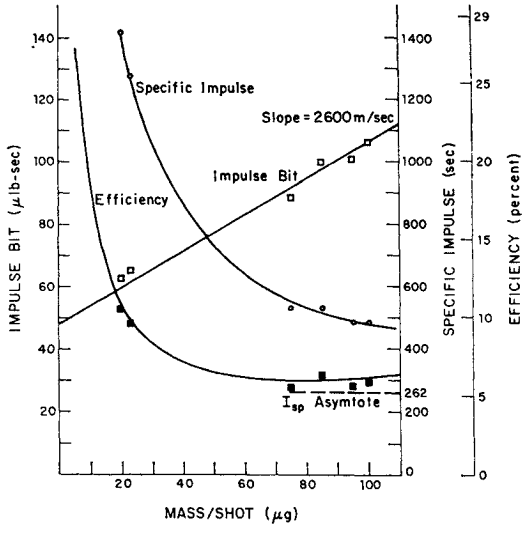

Fig. 6 Performance of 20-joule side feed thruster (with flared electrodes) as a function of mass/shot.

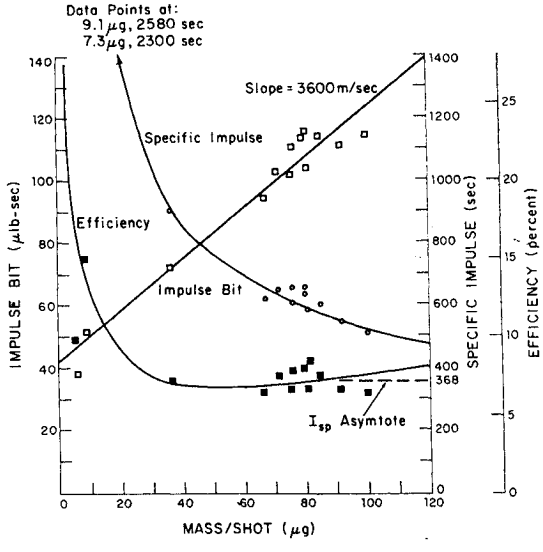

Fig. 7 Performance of 20-joule side feed thruster (with parallel electrodes) as a function of mass/shot.

Finally, the gas-dynamic portion of the thrust was recently calculated for the 2-joule thruster with the conventional back feed.[7] That thruster consumes 7 μg of fuel, so assuming some equivalence with the side-fed thruster consuming the same fuel, we expect the gas-dynamic impulse to equal the magnetic impulse, and that is exactly what was found by calculation from this model.

Ablation and Carbonization

After ~10,000 shots, it was found that portions of each Teflon face became coated with carbon. A typical pattern is shown on the two faces of the fuel in Fig. 8, which have been opened up from their normal configuration to be photographed. When facing each other, the carbon areas are opposite one another, and the exhaust moves from the inside edges (back of the thruster) to the outside edges (the clean area).

One can hypothesize how this pattern developed by assuming the discharge arc curves in its travel from the top electrode (containing the spark plug) to the bottom electrode, burning the Teflon away in the white pattern. The carbon area could form because there is no arc passing over that portion of the Teflon to ionize the carbon atoms deposited there from the exhaust gas. (It takes relatively little energy to break up the C_2F_4 polymer and produce carbon atoms, compared to the amount required to ionize the atoms once they are ablated and dissociated from the surface.)

Explaining the curved path is not too difficult if one determines the electric field pattern and the current path taken by the initial electrons prior to complete breakdown. This is the path the arc will follow initially. The electric field pattern can be determined from a scaled two-dimensional

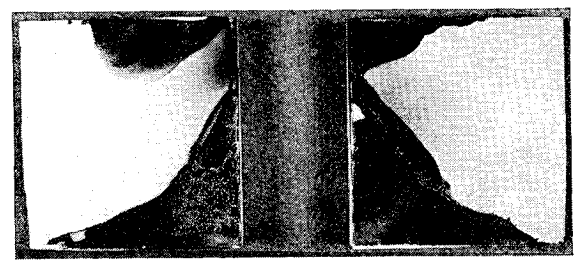

Fig. 8 The faces of the two Teflon side walls after ~10,000 discharges. Thrust is towards the clean end. The cathode is on top and the anode on the bottom. The black area is carbon deposition.

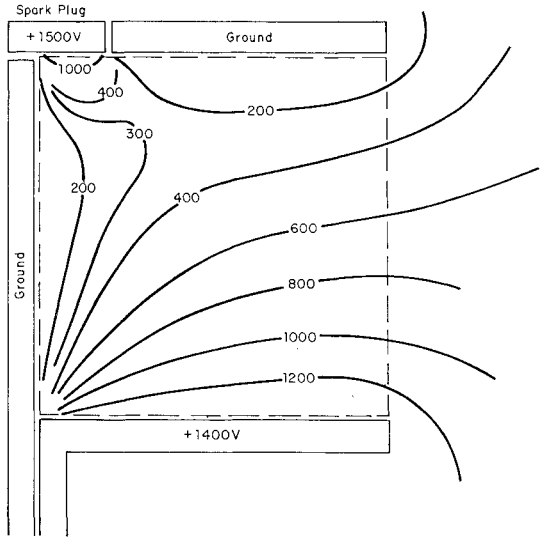

Fig. 9 Potential field lines in nozzle when the back strap is within a few mils of the initial arc discharge.

field plot using teledeltos resistance paper, which yields the potential lines in Fig. 9. Visualizing the gradient of these equipotentials, one can see that the electric field slants forward from the spark plug in the top electrode to the bottom electrode in the region in front of the spark plug. Except for the Hall current produced by the magnetic field as the current increases, the current would follow this forward slant. By moving the back strap away from the spark plug (as in Fig. 10), this slant can be reduced.

The effect of the Hall angle for the configuration of Fig. 10 is shown in Fig. 11. The electron velocity and current are in

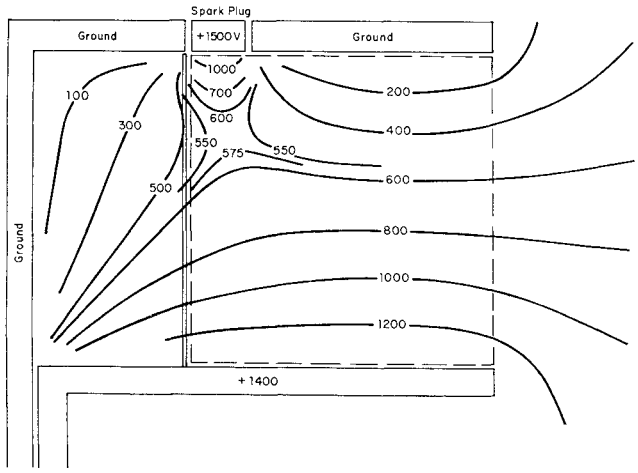

Fig. 10 Potential field lines in the nozzle. The back strap is $\frac{1}{2}$ in. from the initial arc discharge.

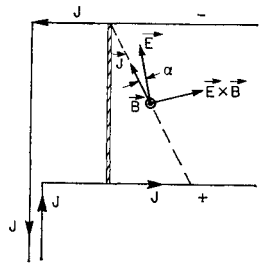

Fig. 11 Electron current direction in the nozzle caused by the $\vec{E}$ and $\vec{E} \times \vec{B}$ forces. α is the Hall angle.

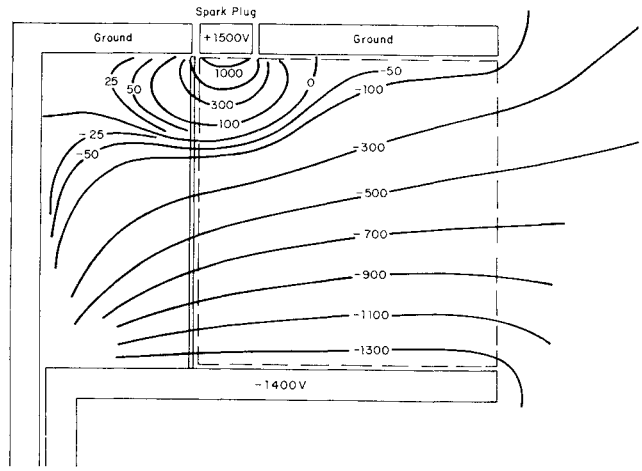

Fig. 12a Potential field lines in the nozzle when the electrode polarity is reversed.

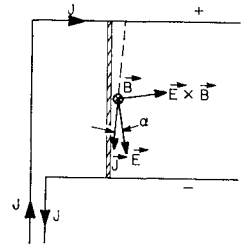

Fig. 12b Electron current direction in the nozzle when the polarity is reversed. α is the Hall angle.

opposite directions, and the velocity is in the plane of E and $E \times B$. With few collisions, the electrons leave the spark plug in the $-E$ direction, but are then curved toward $E \times B$. When collisions dominate, they simply follow $-E$. For intermediate regimes, the Hall angle α gives the current direction with respect to the electric field direction.

To test this hypothesis, we can reverse the polarity of the electrodes in Fig. 10. The new field pattern is shown in Fig. 12a, and the new Hall current (Fig. 12b) now tilts the total current in the direction of the vertical. The result of an experimental test of this idea is shown in Fig. 13 (only the left half of the two faces was photographed, and so thrust is to the left). Apparently the current pattern is indeed vertical.

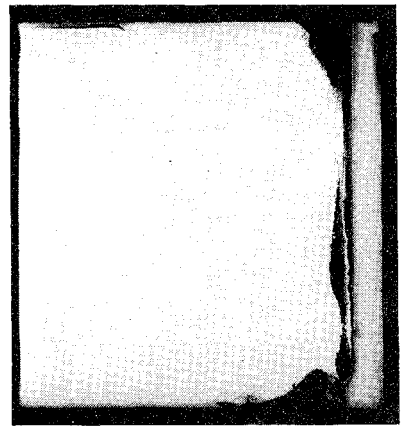

Fig. 13 Carbon deposition pattern for reverse polarity. Thrust is to the left. The cathode is on top and the anode on the bottom. The vertical band on the right behind the carbon is an area not exposed to the discharge.

Summary

A means for improving the performance of a solid fuel pulsed plasma thruster has been described and analyzed. The key to improvement is control over the mass consumed per discharge. Figures 3 and 4 show that the mass consumption can be chosen by adjusting the distance between the two side-fed Teflon fuel bars. For high mass consumption, the thruster operates in the gas-dynamic regime and provides high thrust. At low mass consumption, thruster operation is primarily electromagnetic with high specific impulse. Efficiency increases as the thrust mechanism is predominately in one regime or the other. By using side feed, the performance has been significantly increased over the conventional rear-feed design.

Carbonization of the Teflon side walls remains the one stumbling block to the full utilization of this design to flight thrusters. Geometry changes may reduce or eliminate this problem.

References

[1] Guman, W. J. and Nathanson, D. M., "Pulsed Plasma Microthruster Propulsion System for Synchronous Orbit Satellite," *Journal of Spacecraft and Rockets*, Vol. 7, No. 4, April 1970, pp. 409–415.

[2] Vondra, R., Thomassen, K., and Solbes, A., "Analysis of Solid Teflon Pulsed Plasma Thruster," *Journal of Spacecraft and Rockets*, Vol. 7, No. 12, Dec. 1970, pp. 1042–1406.

[3] Vondra, R., Thomassen, K., and Solbes, A., "A Pulsed Electric Thruster for Satellite Control," *Proceedings of IEEE*, Vol. 59, No. 2, Feb. 1971, p. 271.

[4] Thomassen, K. and Vondra, R., "Exhaust Velocity Studies of a Solid Teflon Pulsed Plasma Thruster," *Journal of Spacecraft and Rockets*, Vol. 9, No. 1, Jan. 1972, pp. 61–64.

[5] Solbes, A. and Vondra, R. J., "Performance Study of a Solid Fuel Pulsed Electric Microthruster," AIAA Paper 72-458, Bethesda, Md., 1972.

[6] Radley, R. J., Jr., "Study of a Pulsed Solid Fuel Microthruster," M.S. thesis, 1969, Dept. of Aeronautics and Astronautics, MIT, Cambridge, Mass.

[7] Thomassen, K. I. and Tong, D., "Interferometric Density Measurements in the Arc of a Pulsed Plasma Thruster," AIAA Paper 72-463, Bethesda, Md., 1972.

OCTOBER 1972 J. SPACECRAFT VOL. 9, NO. 10

Effect of External Radiation on the Burning Rates of Solid Propellants

RALPH L. COATES* AND SOLIM KWAK†

Brigham Young University, Provo, Utah

Experimental data are presented for four different propellants burned inside an electrically heated tube furnace. Pressures ranged from 5 to 20 psia, and furnace temperatures ranged from room temperature to 1750°F. It was observed that under the influence of thermal radiation from the furnace walls, the burning rate of the propellants could be increased by as much as 100%. These data as well as data published recently by others are correlated with a simplified laminar flame theory.

Nomenclature

c_g = heat capacity of gas
F = factor for radiation exchange between nonblack bodies
E_g = activation energy, gas reactions
E_s = activation energy, solid reactions
$\dot{m}$ = mass burning rate ($\dot{m} = r\rho$)
n = burning rate exponent
P = pressure
Q = net radiant flux at burning surface
Q_s = radiant flux emitted by external source
Q_f = see Eq. (8)
r = burning rate
r^0 = burning rate under adiabatic conditions
R = gas constant
T_f = flame temperature
T_f^0 = flame temperature under adiabatic conditions
T_s = temperature of burning surface
T_s^0 = temperature of burning surface under adiabatic conditions
T_∞ = temperature of surroundings
σ = Stefan-Boltzmann constant
ρ = density of solid

Presented as Paper 72-35 at the AIAA 10th Aerospace Sciences Meeting, San Diego, Calif., January 17–19, 1972; submitted January 26, 1972; revision received June 19, 1972. This research was supported by the Air Force Office of Scientific Research under Grant AFOSR-70-1895.

Index categories: Properties of Fuels and Propellants; Combustion in Heterogeneous Media; Solid and Hybrid Rocket Engines.

* Professor, Chemical Engineering Department. Member AIAA.

† Research Assistant, Chemical Engineering Department.

Introduction

IF the burning surface of a solid propellant is adjacent to an insulated part of the rocket motor, the net radiant exchange of thermal energy between the two surfaces may be expected to differ appreciably from the adiabatic condition where the surface is exposed only to the combustion products and additional burning surface. Early in the burn time the insulation may be cooler and absorb radiant energy from the burning surface. Later, the temperature of the insulated surface may be substantially higher than the burning surface, resulting in a flow of radiant energy from the insulation to the propellant. In either case, it may be expected that the burning rate of the propellant would be different than when burning under adiabatic conditions.

The effect of external radiation has been reported by previous investigators. Youngberg and Horton,[1] using a simply-heated stainless-steel tube furnace, investigated the effect of the external radiant energy on the burning rate of A-13 propellant at atmospheric pressure. An external radiant flux of 2 cal/cm²/sec. was observed to increase the burning by 18%.

Using a variable thermal radiation source consisting of a shutter controlled xenon-mercury lamp, Mihlfeith, Baer, and Ryan[2] studied the effect of external radiant energy on the burning rate of several composite solid propellants. Generally, increases of 11%–31% were reported in their study for radiant fluxes in the range from zero to 14.85 cal/cm²/sec.

Ohlemiller and Summerfield[3] have investigated the effect of external radiation on the burning rate of solid propellants